Sensitivity Analysis of Intensity-Modulated Plastic Optical Fiber Sensors for Effective Ageing Detection in Rapeseed Transformer Oil

Ugochukwu Elele , Azam Nekahi * , Arshad Arshad , Kate McAulay , Issouf Fofana

Posted Date: 3 October 2023

doi: 10.20944/preprints202309.2092.v1

Keywords: Ageing; Fiber Optic Sensor; Transformer Oil; Refractive Index; Evanescent Field; Intensity Modulation

Article

Sensitivity Analysis of Intensity-Modulated Plastic Optical Fiber Sensors for Effective Ageing Detection in Rapeseed Transformer Oil

Ugochukwu Elele [1], Azam Nekahi [1]*, Arshad Arshad [1], Kate McAulay [1], and Issouf Fofana [2]

[1] School of Computing, Engineering and Built Environment, Glasgow Caledonian University, Glasgow G4 OBA, UK
[2] Department of Applied Sciences, Université du Québec à Chicoutimi, Saguenay, QC G7H 2B1, Canada
* Correspondence: azam.nekahi@gcu.ac.uk

Abstract: In the realm of power delivery to end-users, transformers are indispensable, with their malfunctions leading to substantial economic, safety, and environmental repercussions. The need for persistent surveillance is accentuated for in-situ oil-filled transformers, given the potential degradation of oil and the emergence of related ageing by-products. As the focus tilts towards online detection methodologies for transformer oil ageing, bypassing challenges associated with traditional offline methods such as sample contamination and misinterpretation, fiber optic sensors are gaining traction due to their compact nature, cost-effectiveness, and resilience to electromagnetic disturbances typical in high-voltage environments. This work delves into the sensitivity analysis of intensity-modulated plastic optical fiber sensors. The investigation encompasses key determinants such as the influence of optical source wavelengths, noise response dynamics, ramifications of varying sensing lengths, and repeatability assessments. Findings underscore that elongating the sensing length detrimentally affects both the linearity response and repeatability, largely attributed to the diminished resistance to external noise. Additionally, the choice of the optical source wavelength proved to be a critical variable in assessing sensor sensitivity.

Keywords: ageing; fiber optic sensor; transformer oil; refractive index; evanescent field; intensity modulation

1. Introduction

Transformers play an indispensable role in power delivery to end-users. Their vital function, combined with their high cost and extensive maintenance, emphasizes their importance. Any malfunction within the transformer system can halt an entire power station, leading to significant economic consequences, potential threats to life, damage to equipment, and environmental implications [1]. Therefore, continuous monitoring of the transformer's state-of-health (SOH) is crucial. In oil-filled transformers, the oil serves essential roles such as cooling, insulating, arc suppression, and acts as a primary indicator of the transformer's operational SOH. Over time, due to factors like transformer loading and thermal stress, the oil deteriorates [2], producing ageing by-products (ABPs) that compromise its physicochemical properties. These ABPs include gases, acids, and sludge [3–5]. Various offline methods, which encompass the chemical, electrical, physical, and spectroscopic techniques [6], are employed to characterize transformer oil. Generally, the methods to detect transformer ageing are categorized as intrusive or non-intrusive, destructive or non-destructive, and offline or online. Among these, non-destructive online techniques are the most advantageous but require the selection of an appropriate sensor [6].

Recent studies underscore the growing attention towards online ageing sensors designed for transformer oil detection, prominently featuring ABP gas sensors [7] , cross-capacitance sensors [8,9], and fiber-optic sensors [10]. Fiber-optic sensors excel due to their insulating properties, resistance to electromagnetic interference, compactness, lightweight design, high sensitivity, broad bandwidth, adaptability in extreme conditions, resilience, and compatibility with remote and distributed sensing applications [10–12]. These sensors are particularly adept at monitoring physical parameters such as strain, temperature, and humidity. Optical fibers are categorically classified based on their material composition (e.g., plastic, glass, polymer, silicon), refractive index profiles, and light propagation

 doi:10.20944/preprints202309.2092.v1

modes. Notably, multimode fibers possess larger diameters facilitating multiple light propagation pathways, while single-mode fibers, with their narrower diameter, allow only a single light wavelength to traverse. Sensitivity responses of these fibers are inherently influenced by their material selection, refractive index, and propagation mode. A study by [13] indicated that silicon fibers, when applied for acidity monitoring, demonstrated enhanced stability and repeatability compared to polymer fibers. Conversely, polymer fibers were noted for their heightened sensitivity and superior flexibility [12,14].

An optical fiber comprises a core, cladding, and coating. The core, made of either glass or plastic, facilitates light transmission. The cladding, with a lower refractive index than the core, ensures light reflects within the core using the principle of total internal reflection [12] , minimizing scattering loss and protecting the core. The coating, typically plastic, offers the fiber environmental and mechanical protection [12]. Optical fiber sensor instrumentation system has three primary elements: the optical transmitter, the sensing region, and the detector. A segment of the optical fiber is stripped to form the sensing area. Light sources can be LEDs or laser diodes. Optical fiber sensors fall into intrinsic or extrinsic categories [12,15]. Intrinsic sensors utilize a stripped section of the optical fiber itself as the sensor, directly interacting with the material being measured to modulate a light property. Extrinsic sensors, however, channel light to an external sensor. Intrinsic sensors dominate in popularity. Intrinsic configurations measure changes in light wave parameters such as wavelength, phase, and intensity. Consequently, optical fiber sensors (OFS) can be phase, intensity, wavelength, or polarization-modulated [12].

In high voltage transformer applications, the adoption of plastic optical fiber sensors has been comparatively under-researched, relative to other offline characterization methodologies. This study distinctively delves into the sensitivity analysis of plastic optical fiber sensors within transformers utilizing rapeseed oil. Subsequent sections elucidate the fundamental principles underpinning the chosen sensor, outline the experimental materials and methodologies employed, analyze the sensitivity of pivotal variables within the instrumentation system, and provide a comprehensive discussion and conclusion on the salient findings. Furthermore, recommendations are presented for enhancing sensitivity in transformer oil applications.

2. Principles of Intensity-Modulated Fibre Optic Instrumentation

When light transitions between different media, its velocity alters, leading to the phenomenon of refraction. Light propagates most rapidly in a vacuum compared to any other medium. The refractive index of a substance, such as water or transformer oil, quantifies the variation in light's velocity as it transitions from a vacuum (or air, for practical purposes) into that substance. This relationship can be mathematically represented as:

$$n = \frac{V_1}{V_2} \tag{1}$$

where n represents the refractive index of the material; V_1 represents the speed of light in a vacuum; V_2 represents the speed of light in a material. The evanescent field absorption-based configuration is a widespread intrinsic sensing technique [16]. The parameter to be detected affects the refractive index of the uncladded portion and prevents optical waves from leaking into the fiber optic waveguide [16] and consequently diminishes some properties of the light wave reaching the fiber output.

Mathematically [16]:

$$\mu = \frac{P_{clad}}{P_{clad} + P_{core}} \cong \frac{4}{3V} \tag{2}$$

μ is the modal fractional power, P_{clad} and P_{core} are the powers carried on the core and cladding, V is the fiber's normalized frequency. The normalized frequency is a unitless quantity expressed as:

$$V = \frac{2\pi a}{\lambda}\sqrt{n^2{}_{core} - n^2{}_{clad}} \tag{3}$$

Preprints (www.preprints.org) | NOT PEER-REVIEWED | Posted: 3 October 2023 doi:10.20944/preprints202309.2092.v1

a is the fiber core radius, λ is the wavelength of the optical source, n_{core} *and* n_{clad} are the refractive indices of the core and cladding respectively. With constant source wavelength, core diameter, and core refractive index, P_{clad} becomes proportionally related to the clad refractive index, n_{clad} (combining equations 2 and 3). The uncladded region (sensing area) makes direct contact with the ageing transformer oil sample, and so n_{clad} becomes replaced with n_{oil}, and P_{clad} is replaced by P_{oil} representing power lost to the transformer oil owing to changes in the refractive index of the oil. This loss modulates the intensity at the end of the optical fiber and forms the basis for inferring the concentrations or purity of the oil in contact with the uncladded section of the optical fiber sensor, due to evanescent field interaction with the oil and the refractive index of the oil [14,17–19].

Optical properties such as light scattering, absorption, reflection, and dispersion are influenced by the refractive index of the medium in which they travel. Consequently, the refractive index is a critical parameter in fiber optic instrumentation. [14,17]. Ageing increases the refractive index of the transformer oil and consequently increases the power lost to the transformer oil. This power will not get to the fiber optic output, thus defining a sensing area (uncladded) that responds to the transformer oil ageing behaviour. Optical fiber sensors have garnered significant traction in sectors such as environmental monitoring, biomedical diagnostics and treatments, biochemical material analysis, and the food industry [14,17].

3. Materials and Methods

3.1. Sample Ageing and Standard

An exhaustive examination of the degradation trajectory of transformer oil—from inception to culmination—necessitates a prolonged span, ranging from fifteen to fifty years, dedicated to natural ageing observation, data acquisition, and data analysis [20]. This timeframe frequently surpasses conventional research periods. Hence, to deeply probe into the ageing phenomenon and its consequential effects on the dielectric properties, there is an imperative need for a condensed, yet representative, replication of the natural ageing dynamics, colloquially referred to as accelerated ageing techniques. These techniques introduce an amalgamation of electrical and environmental stresses that emulate real-world conditions, strictly in alignment with established standards. In this investigation, the ageing procedure of transformer oil adhered to the ASTM D1934-20 protocol [21]. This specific standard elucidates two distinct methodologies for inducing ageing in transformer oil: one devoid of a metal catalyst (Procedure A) and the other incorporating a metal catalyst (Procedure B). Utilizing a metal catalyst, such as copper, serves to amplify the oxidation rate. This research employed Procedure B. To facilitate a nuanced exploration of the contributory roles of copper and paper in hastening the ageing process, the samples were systematically bifurcated into four categories: solely oil (samples 1-9), oil in conjunction with paper (65g, dimensions 7.5cm x 7cm; samples 10-12), oil supplemented with copper (12g/l concentration; samples 13-15), and an amalgamation of oil, paper, and copper (65g paper, 7.5cm x 7cm in size, with a 12g/l copper concentration; samples 16-18).

The apparatus used include:

1. An oven capable of maintaining a constant temperature of 115°C (ASTM D1934-20).
2. Beakers
3. 18 x 1000ml Pyrex Narrow Mouth Conical Flask
4. Natural Ester Transformer Oil (Rapeseed)
5. Ageing Timer
6. Distilled Water

The procedural steps were as follows:

1. Sample containers were meticulously prepared and designated with labels from S1 through S18. Conforming to the guidelines stipulated in ASTM D1934-20 [21], a sampling duration extending a minimum of 96 hours was strictly maintained.
2. A volume of 750ml of pristine rapeseed oil was allocated to the container marked S1. In a parallel manner, 750ml of the identical oil specimen was allocated to each of seventeen (17) uncontaminated, narrow-mouthed conical flasks, culminating in a total of eighteen (18) samples with congruent mass. In adherence to ASTM D1934-20, and incorporating an amplification

Preprints (www.preprints.org) | NOT PEER-REVIEWED | Posted: 3 October 2023 doi:10.20944/preprints202309.2092.v1

coefficient of 2.333', this paralleled the recommended sampling ratio encompassing a 300ml test specimen situated within a 400ml beaker, achieving an insulating depth proximate to 75mm.

3. The temperature of the oven was meticulously calibrated to register 115 ± 1°C, succeeded by a pre-heating intermission spanning 120 seconds.
4. Flasks, bearing labels from S2 through S18, were systematically introduced into the oven. Established sampling intervals were maintained. As a precautionary measure, protective hand gear was employed to mitigate thermal injuries. A structured ageing schedule was punctiliously updated, reflecting the progressive removal of samples.
5. Upon conclusion of the heating cycle, samples were permitted an adequate cooling period, reverting to ambient conditions.
6. The contents housed within flasks S2 to S18 were systematically transferred to their respective, designated containers (see Figure 1). It was imperative to ensure that these containers remained shielded from direct solar exposure.
7. A thorough cleaning regimen was implemented for flasks S2 through S18, involving washing, rinsing, and subsequent drying.

Figure 1. Samples 1-18.

3.2. Refractive Index Measurement

The refractive index (RI) is a significant property that varies in proportion with the ageing of transformer oil, and it also provides insight into the optical characteristics of various instruments [14,17]. In the works of [16], the sensitivity of fiber optic sensor was expressed mathematically as a ratio of the transduced output voltage to the refractive index unit of the samples.

Mathematically:

$$S = \frac{V_{out}}{n} \; [Volts/RIU] \tag{4}$$

Where S represents the sensitivity of the optical fiber sensor, V_{out} represents the fiber optic transduced output voltage, and n represents the refractive index of the test samples.

The apparatus used include:

1. Fresh and Aged Rapeseed Ester Oil
2. Bellingham + Stanley Refractometer
3. Pipette
4. Clean, lint-free cloth
5. Distilled Water
6. Ethanol

The procedural steps were as follows:

1. The refractometer was adjusted to a refractive index value of 1.3333 utilizing distilled water for calibration purposes.
2. Ethanol, applied with a lint-free cloth, was used to meticulously cleanse the prism of the refractometer.
3. A fresh oil specimen was dispensed onto the prism using a pipette.

Preprints (www.preprints.org) | NOT PEER-REVIEWED | Posted: 3 October 2023 doi:10.20944/preprints202309.2092.v1

4. By closing the refractometer's lid, the oil was uniformly distributed across the prism's surface (see Figure 2).
5. The refractive index was ascertained by examining through the device's eyepiece.
6. The process from steps 2 through 5 was reiterated for samples that had undergone ageing.
7. All recorded refractive index values were methodically logged, followed by the thorough cleaning of the refractometer and the testing area.

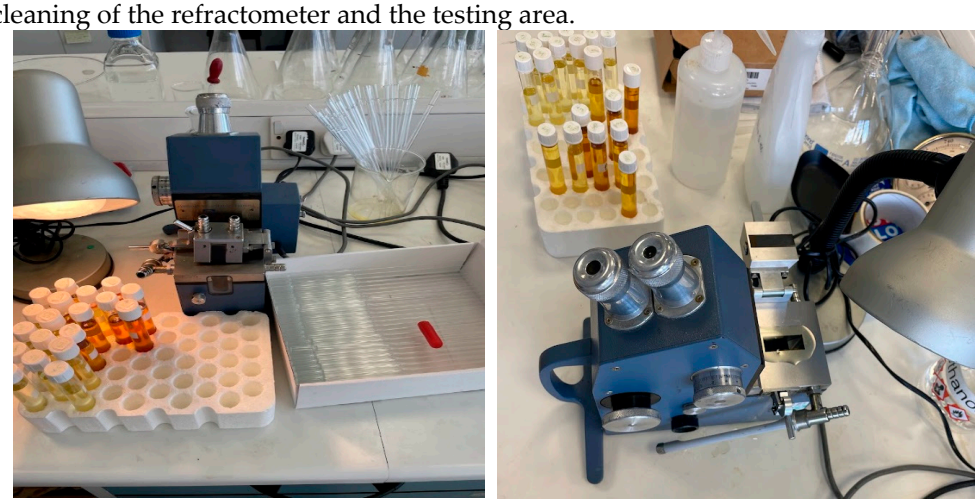

Figure 2. RI Test Bench.

3.3. Fibre Optic Instrumentation Setup and Data Acquisition System

The fiber optic instrumentation apparatus, as delineated in Figure 3, encompasses a step-index polymethyl methacrylate (PMMA) plastic optical fiber (POF), coupled with an optical source, a detector, connector locking nuts, a sample holder, and a data acquisition (DAQ) system.

The designated POF is distinguished by its 1 mm cladding diameter, a core refractive index of 1.492, and a cladding refractive index of 1.41. Through the utilization of a mechanical stripper, sensing lengths of 1.5 cm, 2 cm, and 3 cm were meticulously crafted. These sensing regions were subsequently integrated into both pristine and aged natural ester oil samples, adopting a U-shaped alignment. Notably, this U-shaped arrangement has been demonstrated to exhibit superior sensitivity in comparison to the linear fiber orientation [18]. For the purpose of securing a stable interface between the optical source, the detector, and the optical fiber to the breadboard, connector locking nuts were judiciously employed (refer to Figure 4).

The optical sources consist of 940nm peak wavelength IF-E91A Fiber Optic Infrared Light Emitting Diode (LED), 470nm peak wavelength IF-E92B Fiber Optic Blue LED, 530nm peak wavelength IF-E93 Fibre Optic Green LED, and 645nm peak wavelength IF-E96 Fibre Optic Red LED. The optical fiber detector is a highly sensitive NPN phototransistor (IF-D92). The detector spectral bandwidth ranges from 400nm to 1000nm capable of detecting optical signal from all four sources. The sample holder is an optically insulated container capable of holding up to 127g of the samples.

The microcontroller utilized in this study was the Arduino Mega 2560, responsible for capturing the transduced analog voltage from the phototransistor via its analog input pin (A7). The Arduino microcontroller establishes a connection with the PC-workstation through a USB port, which supplies a peak voltage of 5V DC to the power rails of the Arduino Mega 2560. This regulated voltage was then employed to energize the optical LEDs via current-limiting resistors (refer to Figure 3). With the integration of the MATLAB Support Library for Arduino Hardware, there was an effortless interface between the Arduino Hardware and a PC-workstation equipped with MATLAB software. Data acquisition occurred in real-time, with the data being showcased and archived for subsequent analysis within the MATLAB Simulink Software environment.

Preprints (www.preprints.org) | NOT PEER-REVIEWED | Posted: 3 October 2023 doi:10.20944/preprints202309.2092.v1

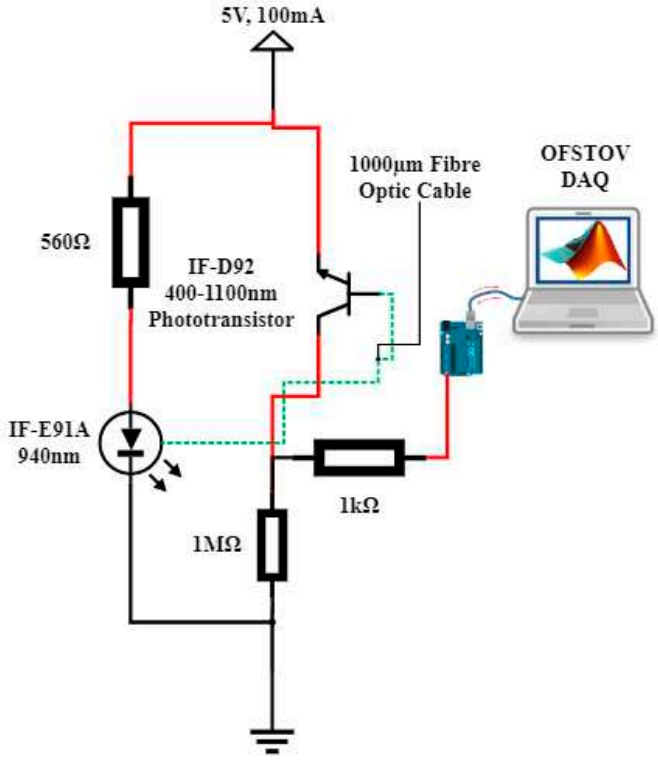

Figure 3. Opto-Electronic Configuration.

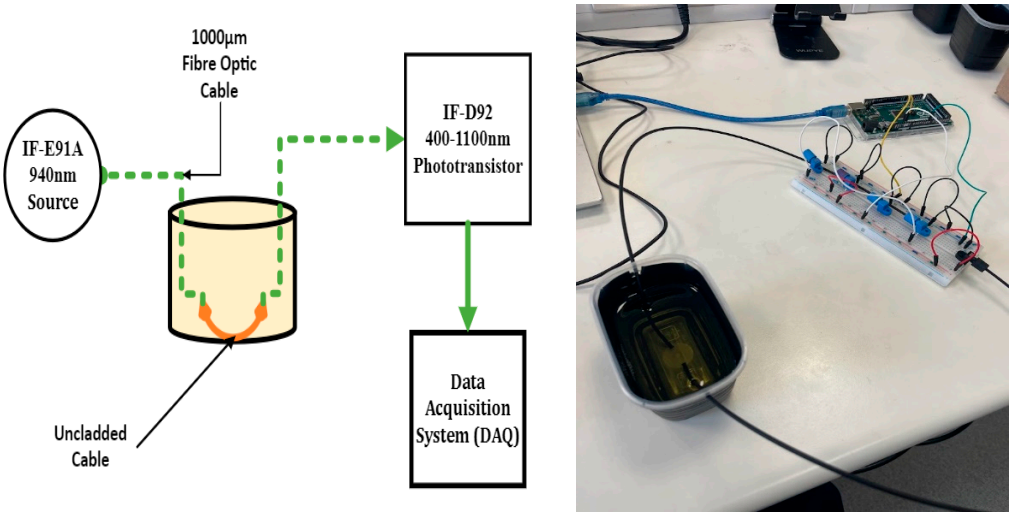

Figure 4. U-Shaped Sensing Configuration.

The apparatus used include:

1. Arduino Mega 2560 microcontroller
2. Light Emitting Diodes (LED) (Infrared, Red, Blue, and Green)
3. Optically Insulated Fabricated vessel for oil
4. 1000µm Uncladded Plastic Fibre Optic Cable
5. Phototransistor
6. Resistors
7. PC Workstation + MATLAB Software
8. Connecting Cables
9. Isopropyl Alcohol

The procedural steps were as follows:

Preprints (www.preprints.org) | NOT PEER-REVIEWED | Posted: 3 October 2023 doi:10.20944/preprints202309.2092.v1

1. The opto-electronic setup was completed as illustrated in Figure 3.
2. The sensing area of the optical fiber sensor was cleaned with isopropyl alcohol to eliminate any contaminants or residual traces of transformer oil.
3. The optical fiber sensor underwent calibration utilizing air for all parameters. The resulting transduced output voltage, as documented in Table 1, served as the calibration reference for deviation adjustments during measurements of both fresh and aged samples.
4. 127g of the fresh oil sample was poured into the optically insulated fabricated vessel.
5. A settling time of one minute was observed before the transduced output voltage time series data were retrieved from MATLAB Simulink.
6. Steps 2 to 5 were repeated for the aged samples.
7. The voltage trend data for all samples were recorded and saved for subsequent analysis.

Table 1. Calibration Voltage.

Sensing Lengths (cm)	LEDs Calibration Voltage (V)			
	Green	Red	Blue	Infrared
1.5	4.99	4.99	4.99	4.9093
2.0	4.99	4.99	4.99	4.7488
3.0	4.99	4.99	4.99	4.1563

4. Results

4.1. Refractive Index Characterisation

The refractive index characterisation trend is shown in Figure 5. The plot shows a positive correlative behaviour between refractive index and the aged samples for all samples. The influence of paper and copper on the refractive index property is also evident in Figure 5. When a trend regression fit is inserted for each of the sample class, the intercept represents the offset or impact of the addition of paper/copper to the ageing process. The influence of paper addition to accelerate the ageing process is seen in the change in the refractive index offset value of 1.3×10^{-3} $[RIU]$ between samples 1-9 and samples 10-12. Copper has a comparatively lower influence of 1×10^{-4} $[RIU]$ between samples 1-9 and samples 13 to 15. The offset between samples 1-9 and samples 16 to 18 is 1.2×10^{-3} $[RIU]$, a little lower than samples 10-12 by 1×10^{-4} $[RIU]$ because of the influence of copper addition, and higher than samples 13 to 15 by 1.1×10^{-3} $[RIU]$.

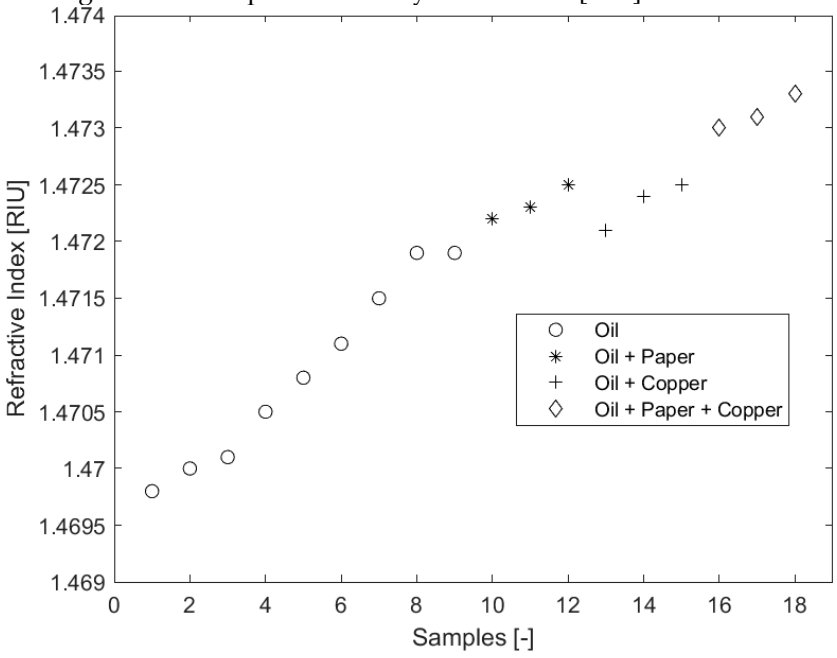

Figure 5. Refractive Index Characterisation with Ageing Trend.

Preprints (www.preprints.org) | NOT PEER-REVIEWED | Posted: 3 October 2023 doi:10.20944/preprints202309.2092.v1

4.2. Sensitivity Analysis

In sensor and instrumentation studies, sensitivity analysis methodically evaluates how input variations impact the measurement system's output. This technique identifies key inputs affecting output, aiding in sensor selection, calibration, and performance troubleshooting. Essentially, sensitivity analysis is vital for understanding and enhancing sensor responsiveness to different conditions or inputs [22].

The key variables under consideration in this study are the impacts of the optical sources wavelengths, noise response analysis, impact of sensing lengths, and repeatability of results.

4.2.1. Impact of Optical Source Wavelengths

Under conditions of constant source power, fixed fiber orientation, and a uniform sensing length of 1.5 cm, data were gathered and averaged across various source inputs featuring different wavelengths for all the samples, as illustrated in Figure 6. One-third of the entire sample sets were utilized in this process. A negative linear trend was anticipated to rationalize the power loss on the cladding, attributable to the absorption within the evanescent field, as well as the corresponding increase in the refractive index, as delineated in Figure 5. The results obtained from the infrared optical source prominently demonstrate this anticipated response. Specifically, the infrared LED source trend manifests a negative linear correlation with the progression of sample ageing, yielding a linear correlation coefficient value of 97.71%. Subsequent to the infrared LED, the red LED displays a faint negative linear correlation with sample ageing, marked by a correlation coefficient value of 6%. Conversely, the green LED reveals a more pronounced positive correlation, a behavior that contravenes the prevailing theoretical understanding. The blue LED exhibits the most attenuated negative correlation among the observed trends.

The observations delineated in Figure 6 can be elucidated further by invoking the principle that optical frequency possesses an inverse relationship with wavelength. This relationship can be expressed mathematically as:

$$c = f\lambda \tag{5}$$

where c represents the speed of the wave, f represents the frequency, and λ represents the wavelength of the wave. As per Planck's quantum theory, mathematically expressed as:

$$E = hf \tag{6}$$

Where E represents the energy of the photon, h represents the Planck's constant which is approximately $6.626 \times 10^{-34}\ joule - seconds$, and f represents the frequency of the photon; the photon energy is proportional to the frequency of the photon. Combining equations 5 and 6, the higher the optical wavelength, the lower the energy. As the infrared LED has the lowest energy, the absorbance will be more [18] leading to a decreased intensity at the detector end.

Preprints (www.preprints.org) | NOT PEER-REVIEWED | Posted: 3 October 2023 doi:10.20944/preprints202309.2092.v1

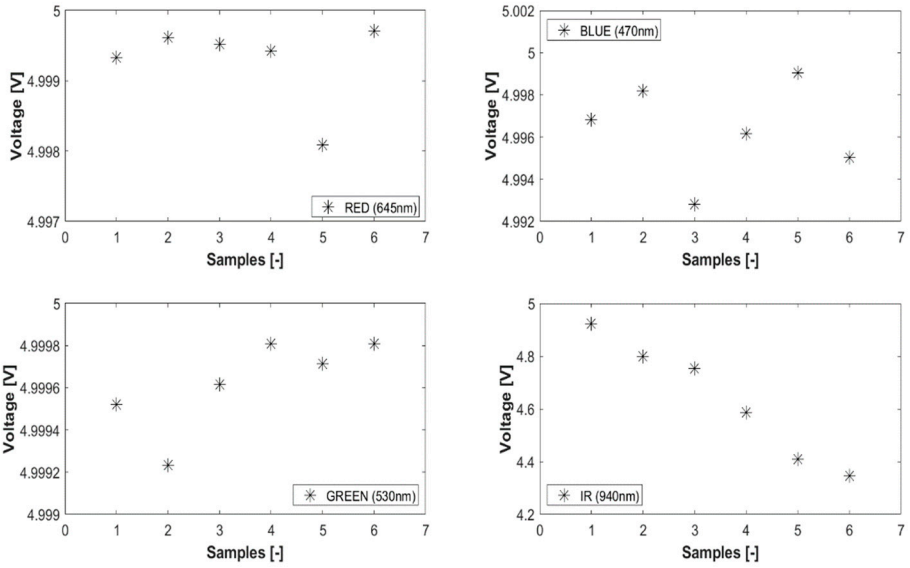

Figure 6. Trend Data from Varying Optical Wavelengths.

4.2.2. Noise Response Analysis

The conducted noise response analysis aimed to evaluate the resilience of the sensors (1.5cm, 2cm, and 3cm) against environmental noise interference. For this assessment, the source voltage to the LEDs was intentionally disconnected, as detailed in Figure 7. Subsequently, the detector's signal mirrored the ambient noise levels as captured by the various optical fiber sensors when they were exposed to air. The visualization of the time-series data and the power spectrum plot was facilitated using MATLAB Live Editor, as depicted in Figures 8 and 9.

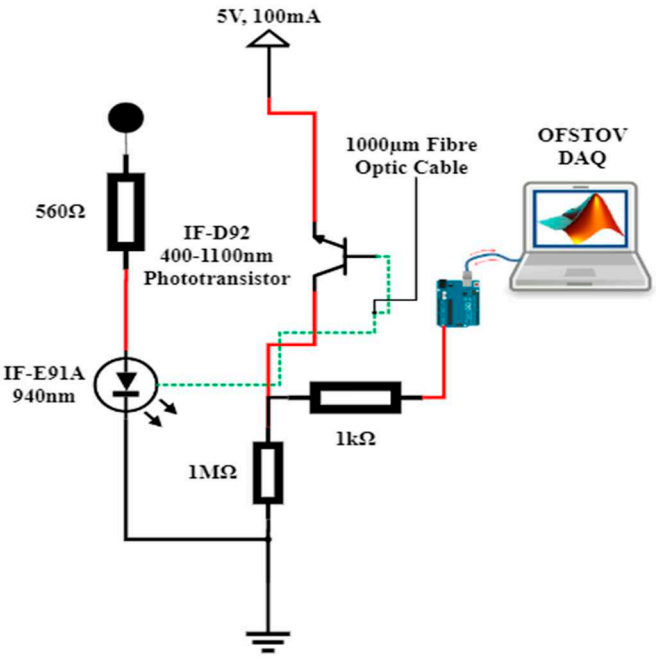

Figure 7. Noise Analysis Opto-Electronic configuration.

Preprints (www.preprints.org) | NOT PEER-REVIEWED | Posted: 3 October 2023 doi:10.20944/preprints202309.2092.v1

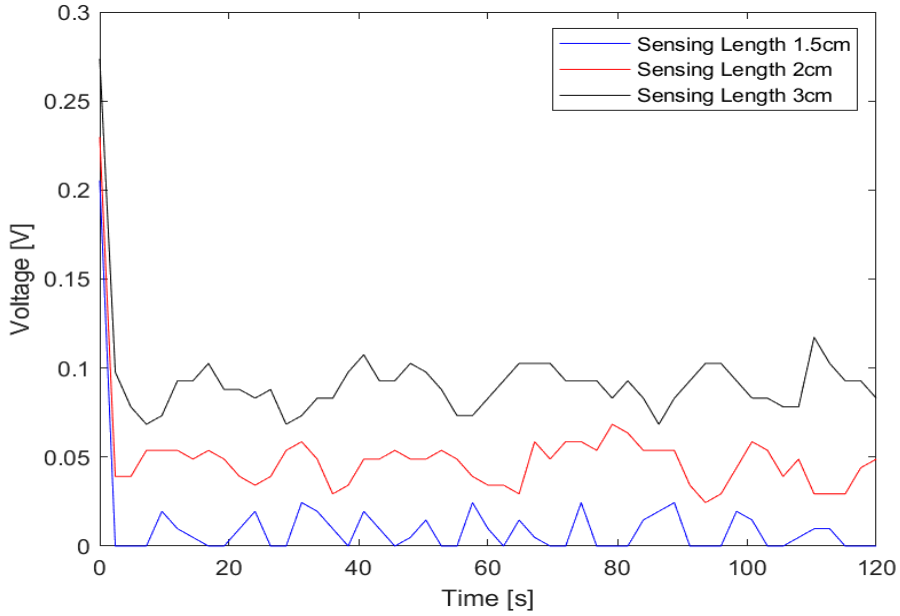

Figure 8. Noise Analysis (Time Series Plot).

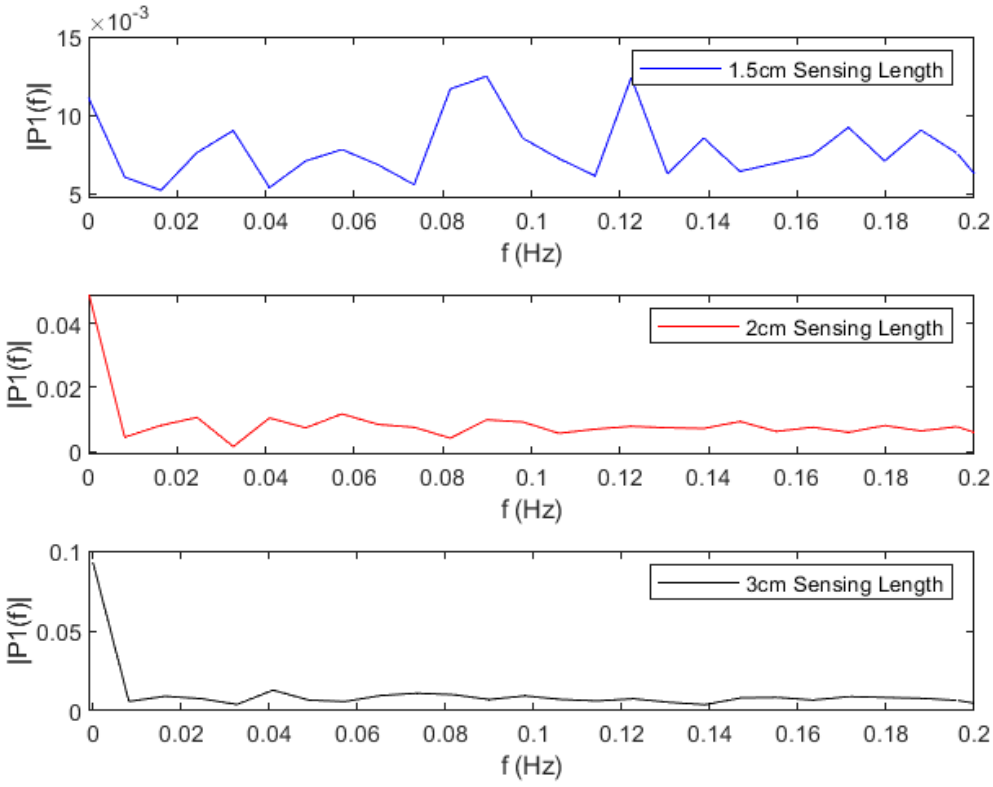

Figure 9. Noise Analysis (Power Spectrum Plot).

Regarding noise amplitude, the sensor featuring a 1.5cm sensing length exhibited the most minimal noise amplitude, succeeded by the 2cm sensor. The 3cm sensor demonstrated the highest amplitude based on the time-series data. This observation aligns with the noise power spectrum plot: the 1.5cm sensor displayed a minimal range of approximately 0.01, followed by the 2cm sensor at 0.04, and the 3cm sensor registering at 0.1. An examination of the noise peaks from the time-series data further indicated that the 1.5cm sensor recorded the fewest peaks.

Preprints (www.preprints.org) | NOT PEER-REVIEWED | Posted: 3 October 2023 doi:10.20944/preprints202309.2092.v1

When considering noise resilience, the 1.5cm sensor consistently demonstrated superior performance in mitigating external noise interference.

4.2.3. Impact of Sensing Lengths

Under consistent parameters including stable source power, invariant fiber orientation, and a set source wavelength of 940nm (as derived from the IF-E91A Fiber Optic Infrared Light Emitting Diode (LED)), an examination was undertaken to understand the implications of different sensing lengths. As delineated in Section 4.2.1, the infrared LED demonstrated optimal performance in alignment with the foundational theoretical framework. As a result, it is favored for this analysis over alternative LED sources.

As illustrated in Figure 10, the sensor's response is influenced by variations in sensing lengths. The effect of noise, as elaborated upon in Section 4.2.2, is evident in the exhibited ageing patterns. The sinusoidal noise trend observed in Figure 8 is mirrored in Figure 10. As the sensing length is extended, the influence of noise becomes increasingly discernible. The sensor with a 1.5cm sensing length boasts a linear correlation coefficient of 94.56%, which is followed by the 2cm sensor with a coefficient of 35.65%, and subsequently, the 3cm sensor registering a value of 0.5%. Notably, the optical fiber with a sensing length of 1.5cm displays optimal linearity, characterized by its descending trend. This trend provides an intuitive representation of the ageing phenomenon and resonates with the instrumentation principles outlined in Section 2.

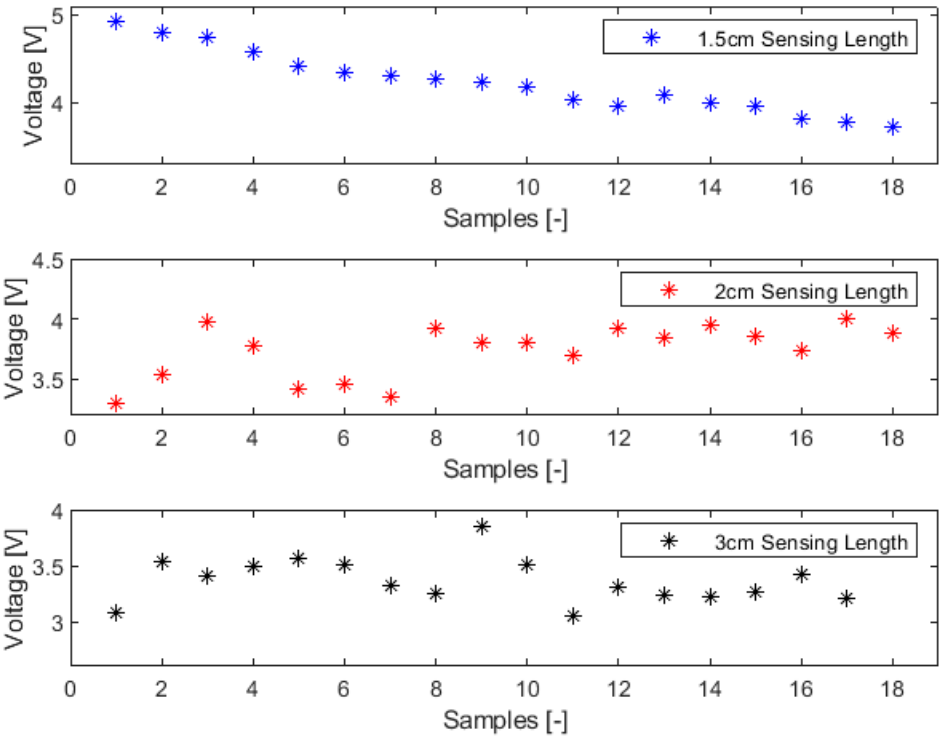

Figure 10. Ageing Trends Based on the Sensing Lengths.

4.3. Repeatability of Results

Repeatability pertains to the degree of agreement among consecutive output readings when a consistent input is administered repetitively over a condensed time interval. This is achieved by maintaining uniform measurement conditions, utilizing the same instrument and observer, and keeping the location and other conditions consistent. As a metric of instrument precision, repeatability serves as an essential index of the reliability of measurement data. For measurement sensors, a high degree of precision in data reporting is not merely an expectation but often a stringent requirement [15].

Preprints (www.preprints.org) | NOT PEER-REVIEWED | Posted: 3 October 2023 doi:10.20944/preprints202309.2092.v1

Repeatability for this work is quoted in terms of the standard deviation of the optical fiber sensor transduced output voltage for three random sample sets (air, sample 1, and sample 5), each comprised of fifty-one transduced voltage values at sampling interval of 2.4 seconds.

Mathematically,

$$\sigma = \sqrt{\frac{1}{n-1}\sum_{i=1}^{n}(V_i - \bar{V})^2} \quad (7)$$

Where σ is the standard deviation, n represents the number of data for each sample, $\bar{V}$ represents the mean of the optical fiber sensor transduced voltage for each sample output voltage, V_i. For repeatability quoted in terms of standard deviation, the smaller the standard deviation, the higher the repeatability. High repeatability can be visualized from the normal distribution curve where the peak is representative of the mean, and the spread of the distribution curve representative of the standard deviation or repeatability. A narrower distribution curve would indicate the desired higher repeatability.

Mathematically, the Gaussian distribution function is expressed as:

$$f(v) = \frac{1}{\sigma\sqrt{2\pi}} e^{-(v-\bar{v})^2/(2\sigma^2)} \quad (8)$$

where f(v) is the probability density function for a given voltage value, v represents the voltage, σ represents the standard deviation.

Under consistent parameters including stable source power, invariant fiber orientation, and a set source wavelength of 940nm, Figures 11 to 14 summarize the repeatability result.

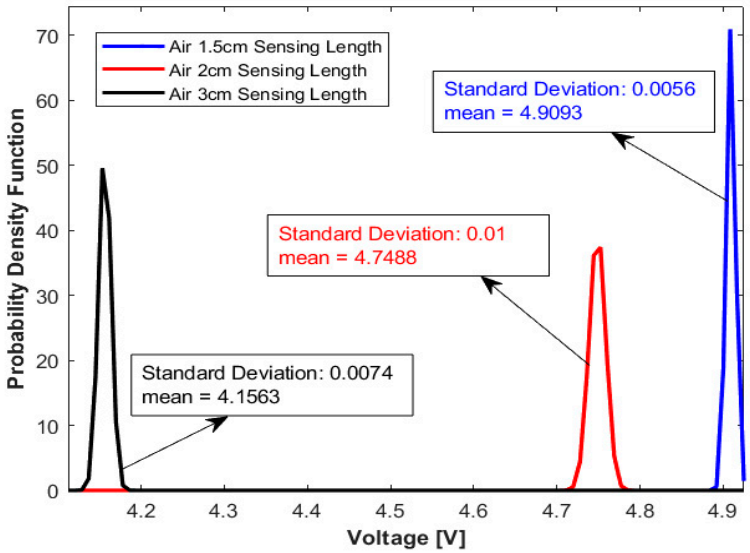

Figure 11. Repeatability Plot of Sensor in Air.

Preprints (www.preprints.org) | NOT PEER-REVIEWED | Posted: 3 October 2023 doi:10.20944/preprints202309.2092.v1

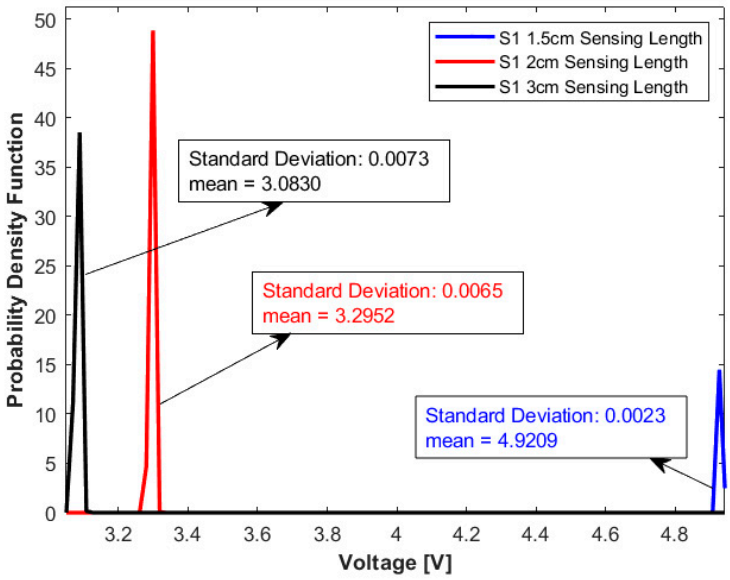

Figure 12. Repeatability Plot of Sensor in Sample, S1.

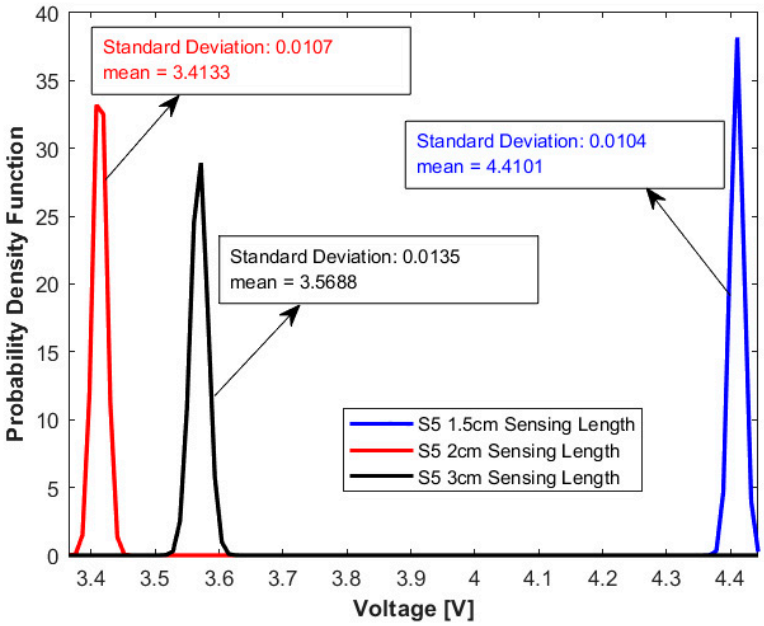

Figure 13. Repeatability Plot of Sensor in Sample, S5.

In a comparative analysis utilizing standard deviation as a metric for repeatability, the optical fiber sensor with a 1.5cm sensing length consistently outperformed its counterparts with longer sensing lengths. This notable distinction in repeatability was consistent across diverse conditions, including ambient air and select aged samples. Given its demonstrated high repeatability, the 1.5cm optical fiber sensor is posited as a more suitable choice for precision-based measurements and advanced instrumentation tasks, compared to the other longer sensing lengths.

5. Discussion, Conclusion, and Future Works

Over the past decades, the deployment of connected digital technologies (sensors and communication systems) in electrical substations has become an important driving force for the digitalization of electrical networks. Sensors deployment is essential to pave the way to digital twining. Continuous monitoring, particularly for oil-filled transformers, is imperative due to

 doi:10.20944/preprints202309.2092.v1

potential oil deterioration and resultant ageing by-products. While various methods exist to characterize transformer oil, non-destructive online techniques are preferred. The rising emphasis is on fiber-optic sensors for detecting transformer oil ageing, given their resistance to interference and heightened sensitivity. These fibers are differentiated by factors like material and light propagation, each with unique benefits. Key elements of an optical fiber sensor system encompass the transmitter, sensing area, and detector, with intrinsic sensors being predominantly used.

In alignment with the principles of intensity-modulated fiber optic sensors and adhering to established industrial aging standards, eighteen samples of rapeseed natural ester oil underwent ageing and were subsequently characterized utilizing a refractometer. The results from the refractive index exhibited a direct linear correlation with the duration of sample ageing. Given the implications of alterations in the refractive index and the evanescent field on the optical fiber sensor, an inverse linear relationship was anticipated and confirmed across several optical sources. Notably, the infrared optical source manifested the most pronounced negative linear correlation, attributed to its reduced optical energy and, consequently, elevated absorbance during sample traversal.

A noteworthy observation is that extending the sensing lengths augmented the sensor's sensitivity to environmental disturbances. The experimental data emphasized that sensors characterized by the shortest sensing lengths exhibited optimal resistance to such environmental perturbations. As a result, the linearity of the optical fiber sensor is intrinsically linked to the length of the sensing region due to potential interference from environmental noise. Consequently, sensors with minimized sensing lengths yielded superior linear outcomes, as evidenced by the correlation coefficient of determination. Further evaluations of repeatability, gauged by the standard deviation, reinforced the superiority of these short-length sensors in terms of repeatability, positioning them as favourable options for precise instrumentation compared to their counterparts with elongated sensing lengths.

Future research trajectories could delve into avenues for enhancing optical fiber sensitivity, potentially by incorporating coatings like agarose. Further investigations might scrutinize the repercussions of diverse intrusive configurations and choice of fiber optic material on sensitivity response. The potential integration of superhydrophobic coatings, aiming to curtail the influence of ageing by-products on sensor sensitivity, also warrants academic exploration. Complementary research endeavors could also pivot towards correlating fiber optic voltage measurements with conventional offline characterization methodologies, fostering the developments and implementation of online ageing models.

Author Contributions: Conceptualization, U.E., A.N., A.A., K.M and I.F.; methodology U.E., resources A.N., A.A., K.M and I.F.; writing—original draft preparation, U.E.; writing—review and editing, U.E., A.N., A.A., K.M and I.F.; supervision A.N., A.A., K.M and I.F.; funding acquisition A.N., A.A., K.M and I.F. All authors have read and agreed to the published version of the manuscript.

Funding: The APC was funded by Glasgow Caledonian University, UK Repository Team.

Institutional Review Board Statement: Not Applicable.

Informed Consent Statement: Not Applicable.

Data Availability Statement: Not Applicable.

Conflicts of Interest: The authors declare no conflict of interest.

Abbreviations

ABP	Ageing By-Products
DAQ	Data Acquisition System
LED	Light Emitting Diode
PMMA	Polymethyl Methacrylic
POF	Plastic Optical Fiber
RI	Refractive Index
SOH	State of Health

References

1. Elele U, Nekahi A, Arshad A, Fofana I. Towards Online Ageing Detection in Transformer Oil: A Review. *Sensors (Basel, Switzerland)* 2022; **22:** 7923.
2. Hadjadj Y, Fofana I, Sabau J, Briosso E. Assessing insulating oil degradation by means of turbidity and UV/VIS spectrophotometry measurements. *IEEE transactions on dielectrics and electrical insulation* 2015; **22:** 2653-2660.
3. Abdelrahman M Alshehawy, Diaa-Eldin A Mansour, Mohsen Ghali, Matti Lehtonen, Mohamed M F Darwish. Photoluminescence Spectroscopy Measurements for Effective Condition Assessment of Transformer Insulating Oil. *Processes* 2021; **9:** 732.
4. Sangineni R, Nayak SK, Becerra M. A Non-intrusive and Non-destructive Technique for Condition Assessment of Transformer Liquid Insulation. *IEEE transactions on dielectrics and electrical insulation* 2022; 1.
5. Ungarala MR, Fofana I, Bétié A, Senoussaoui ML, Brahami M, Briosso E. Condition monitoring of in-service oil-filled transformers: Case studies and experience. 2019.
6. Elele U, Fofana U, Nekahi A, McAulay K, Arshad A. Towards Intrusive Non-Destructive Online Ageing Detection of Transformer Oil Leveraging Bootsrapped Machine Learning Models. 2023; 1-6.
7. Jin L, Kim D, Abu-Siada A, Kumar S. Oil-Immersed Power Transformer Condition Monitoring Methodologies: A Review. *Energies (Basel)* 2022; **15:** 3379.
8. Rahman O, Islam T, Ahmad A, Parveen S, Khera N, Khan SA. Cross Capacitance Sensor for Insulation Oil Testing. *IEEE sensors journal* 2021; **21:** 20980-20989.
9. Rahman O, Islam T, Khera N, Khan SA. A Novel Application of the Cross-Capacitive Sensor in Real-Time Condition Monitoring of Transformer Oil. *IEEE transactions on instrumentation and measurement* 2021; **70:** 1-12.
10. N'cho JS, Fofana I. Review of Fiber Optic Diagnostic Techniques for Power Transformers. *Energies* 2020; **13:** 1789.
11. Mahanta DK, Laskar S. Water Quantity-Based Quality Measurement of Transformer Oil Using Polymer Optical Fiber as Sensor. *IEEE sensors journal* 2018; **18:** 1506-1512.
12. Domingues MdFF, Radwan A. *Optical fiber sensors for IoT and smart devices*. Springer 2017.
13. Riziotis C, El Sachat A, Markos C, Velanas P, Meristoudi A, Papadopoulos A. Assessment of fiber optic sensors for aging monitoring of industrial liquid coolants. Mar 16, 2015; **9359:** 93591Y-8.
14. Teng C, Min R, Zheng J, Deng S, Li M, Hou L, Yuan L. Intensity-Modulated Polymer Optical Fiber-Based Refractive Index Sensor: A Review. *Sensors (Basel, Switzerland)* 2021; **22:** 81.
15. Morris AS, Langari R. *Measurement and instrumentation*. Elsevier:Amsterdam [u.a.], 2021.
16. Hayber ŞE, Tabaru TE, Güçyetmez M. Evanescent Field Absorption-Based Fiber Optic Sensor for Detecting Power Transformer Oil Degradation. *Fiber and integrated optics* 2021; **40:** 229-248.
17. Terdale J, Ghosh A. An intensity-modulated optical fiber sensor with agarose coating for measurement of refractive index. *International journal of system assurance engineering and management* 2022.
18. Patil JJ, Ghosh A. Intensity Modulation based U shaped Plastic Optical Fiber Refractive Index Sensor. *2022 6th International Conference on Trends in Electronics and Informatics (ICOEI)* Apr 28, 2022; 18-24.
19. Khijwania SK, Srinivasan KL, Singh JP. An evanescent-wave optical fiber relative humidity sensor with enhanced sensitivity. *Sensors and actuators. B, Chemical* 2005; **104:** 217-222.
20. Ghosh D, Khastgir D. Degradation and Stability of Polymeric High-Voltage Insulators and Prediction of Their Service Life through Environmental and Accelerated Aging Processes. *ACS omega* 2018; **3** : 11317-11330.
21. ASTM. D1934 Standard Test Method for Oxidative Aging of Electrical Insulating Petroleum Oils by Open-Beaker Method. 2012.
22. Iooss B, Saltelli A. Introduction to Sensitivity Analysis, in: Ghanem R, Higdon D, Owhadi H (Eds.), *Handbook of Uncertainty Quantification*, Springer International Publishing, Cham, 2016;1-20.